Investigation of the characteristics of the intensity noise of singly resonant active second-harmonic generation

Jing Zhang, Yanli Cheng, Tiancai Zhang, Kuanshou Zhang, Changde Xie, and Kunchi Peng

Institute of Opto-Electronics, Shanxi University, Taiyuan 030006, China

Received September 8, 1999; revised manuscript received April 21, 2000

We derive analytical expressions for the quantum-noise spectra of a singly resonant active frequency-doubling laser with single-frequency operation by using a linearized input–output method. For operation of a practical solid-state laser, we analyze separately the contributions of the various noise sources to the final spectrum. The change in resonance in the spectrum from an overdamped- (at higher μ) to an underdamped- (at smaller μ) driven second-order oscillator where μ is the nonlinear coupling coefficient, was experimentally observed with a diode-pumped Nd:YVO_4 + KTP single-frequency-doubling laser. The experimental result is in good agreement with the theoretical expectation. © 2000 Optical Society of America [S0740-3224(00)00410-0]

OCIS code: 270.5290.

1. INTRODUCTION

As compact sources of coherent visible light with high intensity, frequency-doubling solid-state lasers pumped by laser diodes have been attracting interest for various applications. Recent technological progress has made it possible to achieve single-frequency operation of this type of laser with quite low intensity noise.[1,2] The systems that produce several watts of harmonic light are already available from some vendors.

As one of the simplest nonlinear optical processes, passive[3] (occurring in a cavity that is external to a laser) and active (occurring within a laser cavity) second-harmonic generation has been extensively investigated as a source of nonclassical light. The squeezing characteristics of active second-harmonic generation were presented by Collett and Leven.[4] They applied the input–output relation that was originally developed for output coupling through a cavity mirror[5,6] to quadratic coupling between the fundamental and the harmonic, and they predicted that the amplitude noise of the harmonic output could be reduced by 3 dB below the shot-noise level for quite a high pump rate. White *et al.* confirmed this result, using a numerical calculation of the positive P representation, and compared various frequency-doubling systems.[7] The effect of the atomic dephasing rate on squeezing was emphasized.[7] Maeda *et al.* investigated active harmonic amplitude squeezing, considering the spatial evolution of light fields in both a laser medium and a nonlinear crystal.[8]

More recently, linearized input–output approaches were used in a cw atomic laser for which the operator equations of motion were linearized and solved directly, bypassing the master equation.[9,10] In this paper we follow this approach, using the quantum Langevin equation to obtain operator equations of a single-frequency-doubling laser directly from the Hamiltonian. The linearized equations of motion for the quadrature fluctuations in the system are derived from the boundary conditions and solved in Fourier space to yield the amplitude noise spectra. The advantages of this approach are its conceptual simplicity and the presence of analytical solutions in terms of the various noise sources. We obtained, for the first time to our knowledge, the analytical solution of an active singly resonant system rather than merely a numerical calculation as in Ref. 7. Under the condition of a high pump rate, a maximum of 50% squeezing for the amplitude of the second-harmonic wave is predicted at zero frequency, in agreement with previous results. Under the operation conditions of a practical solid-state laser, the contributions of various noise sources to the final noise spectrum are analyzed separately in detail. The change in resonance in the spectrum from an overdamped driven (at higher μ) to an underdamped driven (at smaller μ) second-order oscillator, where μ is the nonlinear coupling coefficient, is experimentally observed with a diode-pumped Nd:YVO_4 + KTP single-frequency-doubling laser. This experimental result is in good agreement with the theoretical calculation.

This paper is arranged as follows: In Section 2 we derive linearized equations for the quantum fluctuations of the single-frequency-doubling laser. In Section 3 the amplitude noise spectra are analyzed. A comparison of calculation results and experimental data is made in Section 4. A brief summary of the paper is presented in Section 5.

2. MODEL OF SINGLY RESONANT ACTIVE SECOND-HARMONIC GENERATION

We consider an active single-frequency-doubling ring laser, as shown in Fig. 1. The laser medium is placed inside the laser cavity. All cavity mirrors have high reflectivity for fundamental frequency ω_0. An optical nonlinear crystal is placed in the path of the cavity field.

0740-3224/2000/101695-09$15.00

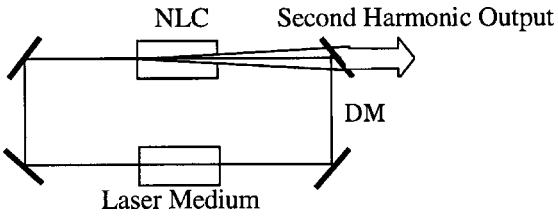

Fig. 1. Single-frequency-doubling ring laser. DM, dichroic mirror (reflectivity, $R \sim 1$ for the fundamental, ~ 0 for the harmonic); NLC, nonlinear crystal.

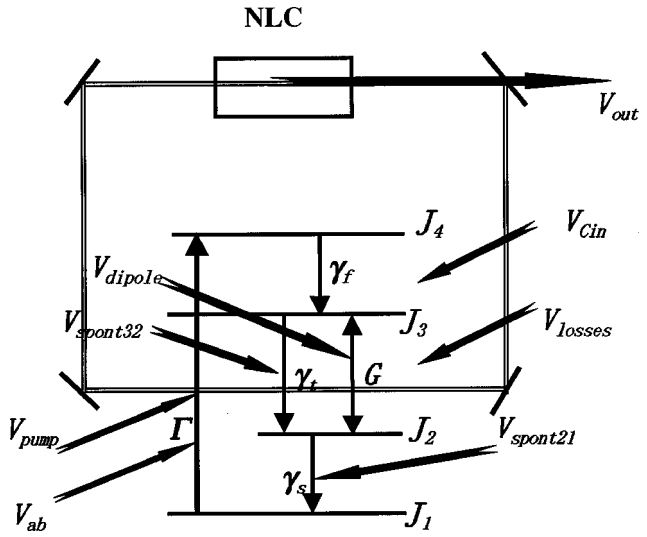

Fig. 2. Diode-pumped single-frequency-doubling laser described by the quantum model: γ_f, γ_t, and γ_s, spontaneous-emission rates; Γ, pump rate; G stimulated-emission coefficient; V_{out}, output harmonic noise; V_{cin}, second-harmonic input noise; V_{pump}, noise entering the laser from its pump source; V_{ab}, quantum (or vacuum) noise, as not all of the pump field is absorbed; V_{spont32}, V_{spont21}, noise from spontaneous emission; V_{dipole}, noise from dipole fluctuations; V_{losses}, noise from intracavity losses; NLC, nonlinear crystal.

The generated harmonic light from the nonlinear crystal passes through one of the cavity mirrors, which is antireflection coated for harmonic frequency $2\omega_0$. To ensure single-mode oscillation, a loss that depends both on polarization and on direction must be introduced. This result is achieved by insertion of a Faraday rotator and a polarization-selecting device such as a Brewster window.

A. Linearized Operator Equations of Motion

We consider the way in which a laser medium consisting of N four-level atoms (see Fig. 2) interacts with two optical cavity modes in a ring cavity. The first mode, represented by the annihilation and creation operators $\hat{a}$ and $\hat{a}^\dagger$, respectively, is the lasing mode with self-energy:

$$\hat{H}_a = \hbar\omega_a \hat{a}^\dagger \hat{a}. \tag{1}$$

It interacts with the active atoms by means of the resonant Jaynes–Cummings Hamiltonian

$$\hat{H}_{\text{laser1}} = i\hbar g(\hat{a}^\dagger \hat{\sigma}_{23} - \hat{a}\,\hat{\sigma}_{23}^+), \tag{2}$$

where circumflexes indicate operators, g is the dipole-coupling strength between the atoms and the lasing mode, and $\hat{\sigma}_{ij}$ and $\hat{\sigma}_{ij}^+$ are the collective Hermitian conjugate atomic lowering and raising operators between the ith and the jth levels. The field phase factors are involved in the definition of the atomic operators. The second mode, $\hat{b}$ and $\hat{b}^\dagger$, is the pump mode with self-energy:

$$\hat{H}_b = \hbar\omega_b \hat{b}^\dagger \hat{b}. \tag{3}$$

It interacts with the active atoms through the resonant Jaynes–Cummings Hamiltonian

$$\hat{H}_{\text{pump2}} = i\hbar g_p(\hat{b}^\dagger \hat{\sigma}_{14} - \hat{b}^\dagger \hat{\sigma}_{14}^+), \tag{4}$$

where g_p is the dipole-coupling strength between the atoms and the pump mode. The third mode, $\hat{c}$ and $\hat{c}^\dagger$, is the second-harmonic mode with self-energy

$$\hat{H}_c = \hbar\omega_c \hat{c}^\dagger \hat{c}. \tag{5}$$

It interacts with the lasing mode through the resonant Jaynes–Cummings Hamiltonian

$$\hat{H}_{\text{shg3}} = i\hbar \frac{\sqrt{u}}{2}(\hat{a}^{\dagger 2}\hat{c} - \hat{a}^2 \hat{c}^\dagger), \tag{6}$$

where $\sqrt{\mu}$ is the dipole coupling strength between the lasing mode and the second-harmonic mode.

The standard techniques of the linearized input–output method[6] are used to couple the lasing atoms and the cavity modes to reservoirs and to derive the operator quantum Langevin equations of motion for the laser. The atomic spontaneous emission from level $|4\rangle$ to level $|3\rangle$, level $|3\rangle$ to $|2\rangle$, and level $|2\rangle$ to $|1\rangle$ is included in our laser model, with rates γ_f, γ_t, and γ_s, respectively. The rates of collisionally or lattice-induced phase decay of the lasing coherence and pump coherence are γ_P and γ_Q, respectively. The laser cavity damping rate that is due to other losses is $2\kappa_l$. The pump mode damping occurs through an input–output mirror with a rate $2\kappa_b$. The cavity decay rate for the second-harmonic mode is $2k_c$. We use $(\hat{a}, \hat{b}, \hat{c}, \hat{\sigma}_{34}, \hat{\sigma}_{23}, \hat{\sigma}_{12}, \hat{\sigma}_3 - \hat{\sigma}_2, \hat{\sigma}_4 - \hat{\sigma}_1)$ for the system operators, $(\delta\hat{A}_l, \hat{B}, \delta\hat{C}, \delta\hat{C}_f, \delta\hat{C}_t, \delta\hat{C}_s, \delta\hat{C}_P$, and $\delta\hat{C}_Q)$ for the input fields, and $(2\kappa_l, 2\kappa_b, 2\kappa_c, \gamma_f, \gamma_t, \gamma_s, \gamma_P, \gamma_Q)$ for the coupling constants.

According to our laser system for singly resonant active SHG, the following assumptions are applied in the calculations:

(i) The pump field decay is rapid (κ_b large), which corresponds to a normally experimental situation without the resonance of pump field.

(ii) The second-harmonic mode decay is rapid (k_c large), consistent with the experimental situation in which the second-harmonic mode is not resonant.

(iii) The upper pump level decay is rapid (γ_f large), which is a desirable condition for efficient pumping and is satisfied in most experimental systems.

(iv) The phase decays of the laser and pump coherences are rapid (γ_P and γ_Q large). This is also a good assumption for most lasers.

These assumptions mean that the pump mode, the upper pump level, and the atomic coherences evolve on much shorter time scales than the other variables. Hence we can make the approximation of adiabatically eliminating the equations for $\hat{b}$, $\hat{c}$, $\hat{\sigma}_4$, $\hat{\sigma}_{14}$ and $\hat{\sigma}_{23}$ by set-

ting their time derivatives to zero. So we obtain the following operator equations of motion for the laser[4,11]:

$$\dot{\hat{a}} = \frac{\tilde{G}}{2}(\hat{\sigma}_3 - \hat{\sigma}_2)\hat{a} - \kappa_l\hat{a} - \mu\hat{a}^\dagger\hat{a}^2 + 2\sqrt{\mu}\hat{a}^\dagger\delta\hat{C} + \sqrt{2\kappa_l}\delta\hat{A}_l - \sqrt{\tilde{G}}\delta\hat{\Lambda}_p, \tag{7}$$

$$\dot{\hat{\sigma}}_1 = -\frac{4G_p\kappa_b\hat{\sigma}_1}{(\kappa_b + 2G_p\hat{\sigma}_1)^2}(\hat{B}^\dagger\hat{B} + \hat{B}\hat{B}^\dagger) + \frac{4G_p\kappa_b}{(\kappa_b + 2G_p\hat{\sigma}_1)^2}(\delta\hat{\Lambda}_q^\dagger\delta\hat{\Lambda}_q + \delta\hat{\Lambda}_q\delta\hat{\Lambda}_q^\dagger) + \sqrt{8G_p\kappa_b}\frac{(\kappa_b - 2G_p\hat{\sigma}_1)}{(\kappa_b + 2G_p\hat{\sigma}_1)^2}(\delta\hat{\Lambda}_q^\dagger\hat{B} + \delta\hat{\Lambda}_q\hat{B}^\dagger) + \gamma_s\hat{\sigma}_2 - \sqrt{\gamma_s}\delta\hat{\Lambda}, \tag{8}$$

$$\dot{\hat{\sigma}}_2 = \frac{\tilde{G}}{2}(\hat{\sigma}_3 - \hat{\sigma}_2)(\hat{a}\hat{a}^\dagger + \hat{\sigma}^\dagger\hat{a}) - \sqrt{\tilde{G}}(\delta\hat{\Lambda}_p\hat{a}^\dagger + \delta\hat{\Lambda}_{pp}^\dagger\hat{a}) + \gamma_t\hat{\sigma}_3 - \gamma_s\hat{\sigma}_2 + \sqrt{\gamma_s}\delta\hat{\Lambda} - \sqrt{\gamma_t}\delta\hat{\Lambda}_t, \tag{9}$$

$$\dot{\hat{\sigma}}_3 = \frac{\tilde{G}}{2}(\hat{\sigma}_3 - \hat{\sigma}_2)(\hat{a}\hat{a}^\dagger + \hat{\sigma}^\dagger\hat{a}) - \sqrt{\tilde{G}}(\delta\hat{\Lambda}_p\hat{a}^\dagger + \delta\hat{\Lambda}_p^\dagger\hat{a}) + \frac{4G_p\kappa_b\hat{\sigma}_1}{(\kappa_b + 2G_p\hat{\sigma}_1)^2}(\hat{B}^\dagger\hat{B} + \hat{B}\hat{B}^\dagger) - \frac{4G_p\kappa_b}{(\kappa_b + 2G_p\hat{\sigma}_1)^2}(\delta\hat{\Lambda}_q^\dagger\delta\hat{\Lambda}_q + \delta\hat{\Lambda}_q\delta\hat{\Lambda}_q^\dagger) - \sqrt{8G_p\kappa_b}\frac{(\kappa_b - 2G_p\hat{\sigma}_1)}{(\kappa_b + 2G_p\hat{\sigma}_1)^2}(\delta\hat{\Lambda}_q^\dagger\hat{B} + \delta\hat{\Lambda}_q\hat{B}^\dagger) - \gamma_t\hat{\sigma}_3 + \sqrt{\gamma_t}\delta\hat{A}_t, \tag{10}$$

where

$$\tilde{G} = \frac{2g^2}{\gamma_P}, \tag{11}$$

$$G_p = \frac{g_p^2}{2\gamma_Q} \tag{12}$$

are the stimulated-emission–absorption rates per photon for the laser and the pump modes, respectively. The noise terms that originate from the various vacuum reservoirs are

$$\delta\hat{\Lambda} = \delta\hat{C}_s^\dagger\hat{\sigma}_{12} + \hat{\sigma}_{12}^+\delta\hat{C}_s = \sqrt{\hat{\sigma}_2}\delta\hat{X}_{C_x}, \tag{13}$$

$$\delta\hat{\Lambda} = \delta\hat{C}_s^\dagger\hat{\sigma}_{23} + \hat{\sigma}_{23}^+\delta\hat{C}t = \sqrt{\langle\hat{\sigma}_3\rangle}\delta\hat{X}_{C_t}, \tag{14}$$

$$\delta\hat{\Lambda}_p = (\delta\hat{C}_P - \delta\hat{C}_P^\dagger)\sigma_{23}, \tag{15}$$

$$\delta\hat{\Lambda}_q = (\delta\hat{C}_Q - \delta\hat{C}_Q^\dagger)\sigma_{14}, \tag{16}$$

$$\delta\hat{\Lambda}_Q = \delta\hat{\Lambda}_q^\dagger + \delta\hat{\Lambda}_q = \sqrt{\langle\hat{\sigma}_1 + \hat{\sigma}_4\rangle}\delta\hat{X}_q, \tag{17}$$

$$\delta\hat{\Lambda}_P = \delta\hat{\Lambda}_p^\dagger + \delta\hat{\Lambda}_p = \sqrt{\langle\hat{\sigma}_3 + \hat{\sigma}_2\rangle}\delta\hat{X}_p. \tag{18}$$

For all these terms the first-order expectation values are zero ($\langle\delta\hat{\Lambda}_i\rangle = 0$). With the operator relationships $\hat{\sigma}_{ij}\hat{\sigma}_{ij}^+ = \hat{\sigma}_i$, $\hat{\sigma}_{ij}^+\hat{\sigma}_{ij} = \hat{\sigma}_j$, and $\hat{\sigma}_{ij}^+\hat{\sigma}_{ij}^+ = \hat{\sigma}_{ij}\hat{\sigma}_{ij} = 0$, the commutator relations between system and input fields, and the properties of the vacuum fields, the following second-order expectation values can be calculated:

$$\langle\delta\hat{\Lambda}(t)\delta\hat{\Lambda}(t')\rangle = \langle\hat{\sigma}_2\rangle\delta(t - t'), \tag{19}$$

$$\langle\delta\hat{\Lambda}_t(t)\delta\hat{\Lambda}_t(t')\rangle = \langle\hat{\sigma}_3\rangle\delta(t - t'), \tag{20}$$

$$\langle\delta\hat{\Lambda}_Q(t)\delta\hat{\Lambda}_Q(t')\rangle = \langle\hat{\sigma}_1 + \hat{\sigma}_4\rangle\delta(t - t'), \tag{21}$$

$$\langle\delta\hat{\Lambda}_P(t)\delta\hat{\Lambda}_P(t')\rangle = \langle\hat{\sigma}_3 + \hat{\sigma}_2\rangle\delta(t - t'). \tag{22}$$

By taking expectation values of Eqs. (7)–(10) and using the semiclassical approximation to factorize the expectation values, we obtain the following laser rate equations:

$$\dot{\alpha} = \frac{G}{2}(J_3 - J_2)\alpha - \kappa_l\alpha - \tilde{\mu}\alpha^*\alpha^2, \tag{23}$$

$$\dot{J}_1 = -\Gamma J_1 + \gamma_s J_2, \tag{24}$$

$$\dot{J}_2 = G(J_3 - J_2)\alpha\alpha^* + \gamma_t J_3 - \gamma_s J_2, \tag{25}$$

$$\dot{J}_3 = -G(J_3 - J_2)\alpha\alpha^* - \gamma_t J_3 + \Gamma J_1, \tag{26}$$

where $\langle\hat{a}\rangle/\sqrt{N} = \alpha$ and $\langle\sigma_i\rangle/N = J_i$ are the expectation values of the laser mode and atomic populations, respectively, in a scaled linear form,

$$\Gamma = \frac{8G_p\kappa_b}{(\kappa_b + 2G_pJ_1)^2}\langle\hat{B}^\dagger\hat{B}\rangle \tag{27}$$

is the pump rate, and

$$\tilde{\mu} = N\mu.$$

Rate G is proportional to stimulated-emission cross section ϵ_s:

$$G = N\tilde{G} = \epsilon_s\rho c,$$

where ρ is the atomic density and c is the speed of light in the medium. Normally one assumes either that the ground state is not significantly depleted by the pumping ($J_1 \approx$ constant) or that the pump beam itself is not significantly depleted [$J_1 \ll \kappa_b/(2G_p)$]. In both cases the pump rate then becomes proportional to the intensity of pump beam. One can obtain the semiclassical steady-state solution by setting the time derivatives to zero in Eqs. (23)–(26).

B. Linearized Fluctuation Equations

In the approximation of a large photon number, we can introduce a quasi-linearization to express $\hat{a}(t)$, $\hat{\sigma}_i(t)$, and $\hat{B}(t)$ as

$$\hat{a}(t) = \sqrt{N}\alpha_0 + \delta\hat{\alpha}(t), \quad \hat{\sigma}_i(t) = NJ_{i0} + \delta\hat{\sigma}_i(t), \quad \hat{B}(t) = \sqrt{N}B_0 + \delta\hat{B}(t), \tag{28}$$

where α_0 and J_{i0} are the semiclassical steady-state solutions of Eqs. (23)–(26) for the laser field amplitude and the population of level i, respectively. B_0 is the coherent amplitude of the pump mode. Without loss of generality we assign α_0 and B_0 as real. The quantum fluctuations

$\delta\hat{a}$, $\delta\hat{\sigma}_i$, and $\delta\hat{B}$ are small and have zero mean. This is normally a good assumption for the magnitude of the laser amplitude. By substituting Eqs. (28) into Eqs. (7)–(10) and retaining only linear terms in the fluctuations we obtain the following set of linear differential equations for the quadrature and population fluctuations:

$$\delta\dot{\hat{X}} = G(\delta\hat{\sigma}_3 - \delta\hat{\sigma}_2)\alpha_0 - \tilde{\mu}\alpha_0^*\alpha_0\delta\hat{X}_a - \tilde{\mu}\alpha_0^2\delta\hat{X}_a + \sqrt{2\kappa_l}\delta\hat{X}_{A_l} + 2\sqrt{\tilde{\mu}}\alpha_0^*\delta\hat{X}_c - \sqrt{G(J_3 + J_2)}\delta\hat{X}_p, \tag{29}$$

$$\delta\dot{\hat{\sigma}}_1 = -\Gamma\sqrt{1-\eta}\delta\hat{\sigma}_1 + \gamma\delta\hat{\sigma}_2 - \sqrt{\Gamma J_{10}\eta}\delta\hat{X}_B + \sqrt{\gamma_s J_2}\delta\hat{X}_{C_x} + [\Gamma(1-\eta)(J_4 + J_1)]^{1/2}\delta\hat{X}_q, \tag{30}$$

$$\delta\dot{\hat{\sigma}}_2 = G(\delta\hat{\sigma}_2)\alpha_0^2 + G(J_{30} - J_{20})\alpha_0\delta\hat{X}_a + \gamma_t\delta\hat{\sigma}_3 - \gamma\delta\hat{\sigma}_2 + \sqrt{\gamma_s J_2}\delta\hat{X}_{C_x} - \sqrt{\gamma_t J_3}\delta\hat{X}_{C_t} - \sqrt{G(J_3 + J_2)}\alpha_0\delta\hat{X}_p, \tag{31}$$

$$\delta\dot{\hat{\sigma}}_3 = -G(\delta\hat{\sigma}_3 - \delta\hat{\sigma}_2)\alpha_0^2 - G(J_{30} - J_{20})\alpha_0\delta\hat{X}_a - \gamma_t\delta\hat{\sigma}_3 + \Gamma\sqrt{1-\eta}\delta\hat{\sigma}_1 + \sqrt{\Gamma J_1\eta}\delta\hat{X}_B + \sqrt{\gamma_s J_2}\delta\hat{X}_{C_x} - [\Gamma(1-\eta)(J_4 + J_1)]^{1/2}\delta\hat{X}_q + \sqrt{\gamma_t J_3}\delta\hat{X}_{C_t} + \sqrt{G(J_3 + J_2)}\alpha_0\delta\hat{X}_p, \tag{32}$$

where the quadrature amplitude fluctuations of the fields are defined by

$$\delta\hat{X}_a = \delta\hat{\alpha} + \delta\hat{\alpha}^\dagger, \quad \delta\hat{X}_{A_l} = \delta\hat{A}_l + \delta\hat{A}_l^\dagger,$$
$$\delta\hat{X}_c = \delta\hat{C} + \delta\hat{C}^\dagger \ldots. \tag{33}$$

Also, we have

$$\sqrt{1-\eta} = \frac{\kappa_b - 2G_pJ_{10}}{\kappa_b + 2G_pJ_{10}}, \tag{34}$$

$$\eta = \frac{8G_pJ_{10}\kappa_b}{(2G_pJ_{10} + \kappa_b)^2}. \tag{35}$$

η is the efficiency with which pump light is absorbed by the lasing atoms. The boundary condition of the second-harmonic output field[3] is

$$\hat{C}_{\text{out}} = \sqrt{\mu}\hat{a}^2 - \delta\hat{C}_m, \tag{36}$$

where $\hat{C}_{\text{out}}$ is the second-harmonic output field. The amplitude quadrature fluctuation is

$$\delta\hat{X}_{C_{\text{out}}} = 2\sqrt{\tilde{\mu}}\alpha_0\delta\hat{X}_a - \delta\hat{X}_c. \tag{37}$$

3. NOISE SPECTRA OF THE SECOND-HARMONIC OUTPUT FIELD

A. Solutions of the Second-Harmonic Noise Spectrum

In frequency space one can solve Eqs. (29)–(32) for the quadrature fluctuations of the output fields by using Eq. (37); hence the expression for the quadrature amplitude fluctuations of second-harmonic output is obtained in terms of the input field fluctuations

$$\delta X_{C_{\text{out}}} = \{[2\tilde{\mu}\alpha_0^2 - i\omega - F1(\omega)]\delta X_c + 2\sqrt{\tilde{\mu}}\alpha_0\sqrt{\Gamma J_1}F2(\omega)\sqrt{(1-\eta)}\delta X_q + 2\sqrt{\tilde{\mu}}\alpha_0\sqrt{\Gamma J_1}F2(\omega)\sqrt{\eta}\delta X_B + 2\sqrt{\tilde{\mu}}\alpha_0\sqrt{\gamma_s J_2}F3(\omega)\delta X_{C_x} + 2\sqrt{\tilde{\mu}}\alpha_0\sqrt{\gamma_t J_3}F4(\omega)\delta X_{C_t} + 2\sqrt{\tilde{\mu}}\alpha_0\sqrt{G(J_3 + J_2)}[1 - F4(\omega)]\delta X_p + 2\sqrt{\tilde{\mu}}\alpha_0\sqrt{2k_l}\delta X_{A_l}\}/[i\omega + F1(\omega) + 2\tilde{\mu}\alpha_0^2]\}, \tag{38}$$

where the absence of the circumflexes indicate Fourier transforms and

$$F1(\omega) = \frac{G^2a_0^2(J_3 - J_2)(2i\omega + \gamma_s + 2\tilde{\Gamma})}{(i\omega + \tilde{\Gamma})(i\omega + \gamma_s + 2Ga_0^2 + \gamma_t) + \gamma_s(Ga_0^2 + \gamma_t)}, \tag{39}$$

$$F2(\omega) = \frac{Ga_0(i\omega + \gamma_s - \gamma_t)}{(i\omega + \tilde{\Gamma})(i\omega + \gamma_s + 2Ga_0^2 + \gamma_t) + \gamma_s(Ga_0^2 + \gamma_t)}, \tag{40}$$

$$F3(\omega) = \frac{Ga_0(i\omega + 2\tilde{\Gamma} + \gamma_t)}{(i\omega + \tilde{\Gamma})(i\omega + \gamma_s + 2Ga_0^2 + \gamma_t) + \gamma_s(Ga_0^2 + \gamma_t)}, \tag{41}$$

$$F4(\omega) = \frac{Ga_0(i\omega + 2\tilde{\Gamma} + \gamma_s)}{(i\omega + \tilde{\Gamma})(i\omega + \gamma_s + 2Ga_0^2 + \gamma_t) + \gamma_s(Ga_0^2 + \gamma_t)}, \tag{42}$$

where $\tilde{\Gamma} = \Gamma\sqrt{1-\eta}$. The second-harmonic amplitude noise spectrum (V_{out}) is

$$V_{\text{out}}(\omega) = \langle|\delta X_{\text{out}}|^2\rangle = \{[2\tilde{\mu}\alpha_0^2 - i\omega - F1(\omega)]^2V_{\text{cin}} + 4\tilde{\mu}\alpha_0^2\Gamma J_1[F2(\omega)]^2(1-\eta)V_{ab} + 4\tilde{\mu}\alpha_0^2\Gamma J_1[F2(\omega)]^2\eta V_{\text{pump}} + 4\tilde{\mu}\alpha_0^2\gamma_s J_2[F3(\omega)]^2V_{\text{spont21}} + 4\tilde{\mu}\alpha_0^2\gamma_t J_3[F4(\omega)]^2V_{\text{spont32}} + 4\tilde{\mu}\alpha_0^2G(J_3 + J_2)[1 - F4(\omega)]^2V_{\text{dipole}} + 8\tilde{\mu}\alpha_0^2k_lV_{\text{losses}}\}/[i\omega + F1(\omega) + 2\tilde{\mu}\alpha_0^2]^2, \tag{43}$$

where brackets stand for absolute squares. A variety of noise sources in Eq. (43) is separately expressed term by term, V_{cin} is second-harmonic input noise, V_{ab} is quantum (or vacuum) noise that is due to the pump field's not being completely absorbed, V_{pump} is pump source intensity

noise, V_{spont21} is spontaneous-emission noise from level $|2\rangle$ level to $|1\rangle$, V_{spont32} is spontaneous-emission noise from level $|3\rangle$ to $|2\rangle$, V_{dipole} is the dipole fluctuation noise between levels $|3\rangle$ and $|2\rangle$, and V_{losses} is noise introduced from intracavity losses. The second-harmonic amplitude noise spectrum V_{out} is normalized to the QNL. $V_{\text{out}} = 1$ indicates QNL operation. The quantum-noise sources are all at this level; i.e., $V_{\text{cin}} = V_{\text{ab}} = V_{\text{spont21}} = V_{\text{spont32}} = V_{\text{losses}} = 1$. However, the pump noise spectrum V_{pump} is arbitrary.

B. Intensity-Noise Characteristics of Second-Harmonic Output from a Singly Resonant Active Frequency-Doubling Laser

We first consider the limit in which the losses are negligible, $\gamma_t \simeq \kappa_l \simeq 0$, and the laser operates well above threshold, $G\alpha_0^2 \gg \Gamma, \tilde{\mu}a_0^2, \gamma_s$. In this limit Eq. (43) is reduced to the following expression:

$$V_{\text{out}}(\omega) = \frac{\omega^2}{\omega^2 + (4\tilde{\mu}\alpha_0^2)^2} + \frac{2(2\tilde{\mu}\alpha_0^2)^2(\omega^2 + \gamma_s^2)}{[4\tilde{\mu}\alpha_0^2(\gamma_s + 2\tilde{\Gamma}) - 2\omega^2]^2 + \omega^2(8\tilde{\mu}\alpha_0^2 + \gamma_s + 2\tilde{\Gamma})^2} \times [(1 - \eta) + \eta V_{\text{pump}}] + \frac{2(2\tilde{\mu}\alpha_0^2)^2[\omega^2 + (2\tilde{\Gamma})^2]}{[4\tilde{\mu}\alpha_0^2(\gamma_s + 2\tilde{\Gamma}) - 2\omega^2]^2 + \omega^2(8\tilde{\mu}\alpha_0^2 + \gamma_s + 2\tilde{\Gamma})^2}. \quad (44)$$

In Eq. (44), only those noise terms that are due to the vacuum field input at the mirror (first term), noise from the pump source (second term), and spontaneous-emission noise caused by decay from the lower lasing level (third term) are significant. Consider the situation in which the decay from the lower lasing level is much faster than the second-harmonic conversion rate and the pump rate, $\gamma_s \gg \Gamma, \tilde{\mu}a_0^2$. Again Eq. (44) is reduced to

$$V_{\text{out}}(\omega) = \frac{\omega^2}{\omega^2 + (4\tilde{\mu}\alpha_0^2)^2} + \frac{2(2\tilde{\mu}\alpha_0^2)^2}{(4\tilde{\mu}\alpha_0^2)^2 + \omega^2} \times [(1 - \eta) + \eta V_p]. \quad (45)$$

The contribution from the lower-lasing-level decay is negligible. If the pump is quantum-noise limited, $V_{\text{pump}} = 1$, from Eq. (45) the maximum of 50% squeezing for the amplitude of the second-harmonic wave is obtained at zero frequency and decreases along with the increase of analyzed frequency, as shown in Fig. 3. This result is in agreement with that predicted[4,5] at the ideal laser limit.

Now we consider typical gas and solid-state lasers operating close to threshold (in the same order of power). Hence to study their intensity-noise characteristics we abandon the approximation of Eq. (44) and adopt the approximation that the decay rate of the lower lasing level is the most rapid, $\gamma_s \gg \gamma_t, \Gamma, G\alpha_0^2$. In this limit we get the following expression for the spectrum:

$$V_{\text{out}}(\omega) = (\{[2\tilde{\mu}a_0^2(Ga_0^2 + \tilde{\Gamma} + \gamma_t) + \omega^2 - 2Ga_0^2(\tilde{\mu}a_0^2 + \kappa_l)]^2 + \omega^2(2\tilde{\mu}a_0^2 - Ga_0^2 - \tilde{\Gamma} - \gamma_t)^2\} + \{4\tilde{\mu}\alpha_0^2\Gamma J_1 G^2 a_0^2[1 + \eta(V_{\text{pump}} - 1)]\} + (4\tilde{\mu}\alpha_0^2\gamma_t J_3 G^2 a_0^2) + \{4\tilde{\mu}\alpha_0^2 G(J_3 + J_2)[(\gamma_t + \tilde{\Gamma})^2 + \omega^2]\} + \{8\tilde{\mu}\alpha_0^2 k_l[(Ga_0^2 + \tilde{\Gamma} + \gamma_t)^2 + \omega^2]\})/[(\omega_r^2 - \omega^2)^2 + \omega^2(\gamma_L)^2]; \quad (46)$$

$$\omega_r = [2\tilde{\mu}a_0^2(Ga_0^2 + \tilde{\Gamma} + \gamma_t) + 2Ga_0^2(\tilde{\mu}a_0^2 + \kappa_l)]^{1/2}, \quad (47)$$

$$\gamma_L = 2\tilde{\mu}a_0^2 + Ga_0^2 + \tilde{\Gamma} + \gamma_t, \quad (48)$$

where ω_r indicates the resonant frequency in the spectrum and γ_L is the damping rate of the oscillations. If the resonance-driven second-order oscillator is underdamped ($\omega_r > \gamma_L$), an oscillation known as resonant relaxation oscillation (RRO) is produced. If the resonance is overdamped ($\omega_r < \gamma_L$), the oscillation is suppressed. Compared with the single-frequency-doubling laser, the single-frequency laser that has no nonlinear crystal in the laser cavity extracts the fundamental field ω_0 from output coupling mirror (k_m) instead of from nonlinear coupling $\tilde{\mu}a_0^2$. We can see from Eqs. (23)–(26) and (36) that, if output coupling mirror k_m equals nonlinear conversion $\tilde{\mu}a_0^2$ and the other parameters do not change, the output power of the single-frequency laser is equal to the single-

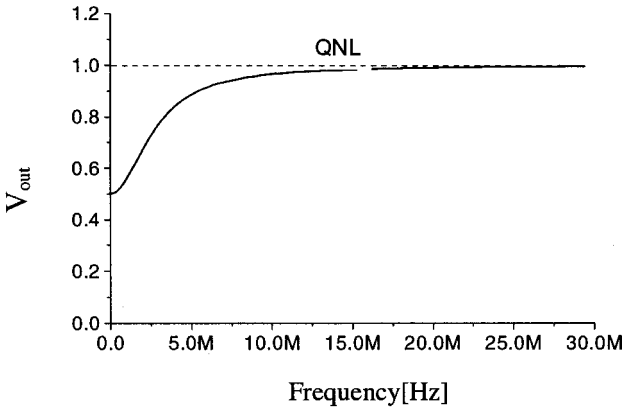

Fig. 3. Spectra of the output harmonic field in the limit well above threshold. $V_{\text{pump}} = 1$, $\mu\alpha_0^2 = 4.27 \times 10^6\ \text{s}^{-1}$.

Table 1. Parameters of a Nd:YVO_4 Single-Frequency-Doubling Ring Laser

Length of cavity	L	350 mm
Single-pass losses	δ_{cav}	3%
Maximum pump power	P_{max}	1 W
Decay rate of intracavity losses	k_1	$1.28 \times 10^7\ \text{s}^{-1}$
Number of lasing atoms	N	10^{17}
Decay rate of upper laser level	γ_t	$10^4\ \text{s}^{-1}$
Decay rate of lower lasing level	γ	$3.3 \times 10^7\ \text{s}^{-1}$
Simulated emission rate per photon	G	$1 \times 10^{11}\ \text{s}^{-1}$
Maximum pump rate	Γ	$8\ \text{s}^{-1}$
Nonlinear conversion rate	$\tilde{\mu}$	$2 \times 10^{13}\ \text{s}^{-1}$

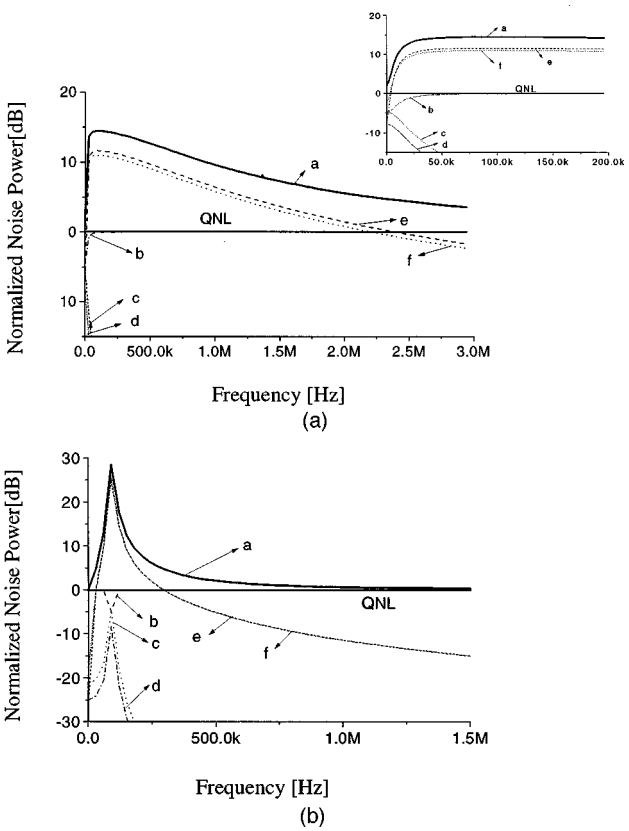

Fig. 4. Frequency dependence of the various noise sources. (a) Resonance overdamped ($\omega_r < \gamma_r$), with $\tilde{\mu} = 2 \times 10^{13}\,\mathrm{s}^{-1}$; (b) resonance underdamped ($\omega_r > \gamma_r$) with $\tilde{\mu} = 2 \times 10^{11}\,\mathrm{s}^{-1}$; other parameters, those in Table 1 with $V_{\mathrm{pump}} = 1$. a, Noise of the harmonic with all contributions added; b, contribution from V_{Cin}; c, contribution from V_{pump}; d, contribution from V_{spont32}; e, shows the contribution from V_{dipole}; f, contribution from V_{losses}.

frequency-doubling laser. The intensity-noise spectrum of the single frequency is described by the following expression[10]:

$$\begin{aligned} V_{\mathrm{out}}(\omega) = (\{&[2k_m(Ga_0^2 + \tilde{\Gamma} + \gamma_t) \\ &+ \omega^2 - 2k_m(\tilde{\mu}a_0^2 + \kappa_l)]^2 \\ &+ \omega^2(2k_m - Ga_0^2 - \tilde{\Gamma} - \gamma_t)^2\} \\ &+ \{2k_m\Gamma J_1 G^2 a_0^2[1 - \eta(V_{\mathrm{pump}} - 1)]\} \\ &+ (2k_m\gamma_t G^2 a_0^2 J_3) \\ &+ \{2k_m G(J_3 + J_2)([\gamma_t + \tilde{\Gamma})^2 + \omega^2]\} \\ &+ \{4k_m k_l[(Ga_0^2 + \tilde{\Gamma} + \gamma_t)^2 + \omega^2]\})/ \\ &[(\omega_r'^2 - \omega^2)^2 + \omega^2(\gamma_L')^2], \end{aligned} \tag{49}$$

where the frequency of the RRO ω_r' is

$$\omega_r' = [2Ga_0^2(k_m + \kappa_l)]^{1/2} \tag{50}$$

and damping rate γ_l' is

$$\gamma_l' = Ga_0^2 + \tilde{\Gamma} + \gamma_t. \tag{51}$$

Comparing Eqs. (46) and (49) shows that the numerators of the first term (vacuum noise input) are identical, the numerators of the second to fifth terms differ by a factor 2, and the common denominators are widely different. The intensity-noise spectrum of the single-frequency laser

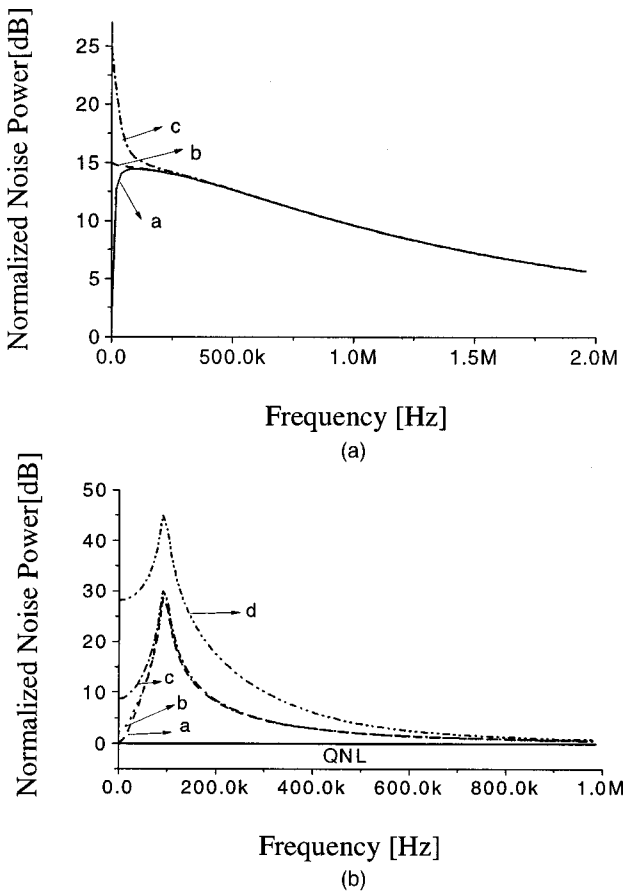

Fig. 5. Harmonic spectra for different pump noise from that of Fig. 4(a). Resonance overdamped ($\omega_r < \gamma_r$), with $\tilde{\mu} = 2 \times 10^{13}\,\mathrm{s}^{-1}$; (b) resonance underdamped ($\omega_r > \gamma_r$), with $\tilde{\mu} = 2 \times 10^{11}\,\mathrm{s}^{-1}$. a, curve a pump noise $V_{\mathrm{pump}} = 1$; b, $V_{\mathrm{pump}} = 20$ dB; c, $V_{\mathrm{pump}} = 30$ dB; d $V_{\mathrm{pump}} = 50$ dB.

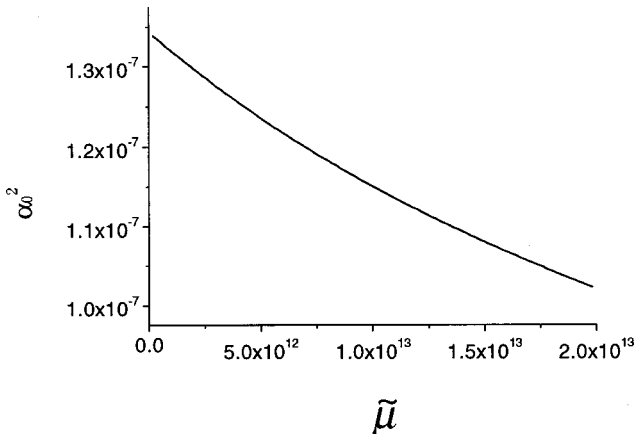

Fig. 6. Intracavity fundamental photon number α_0^2 per atom of the lasing mode versus $\tilde{\mu}$.

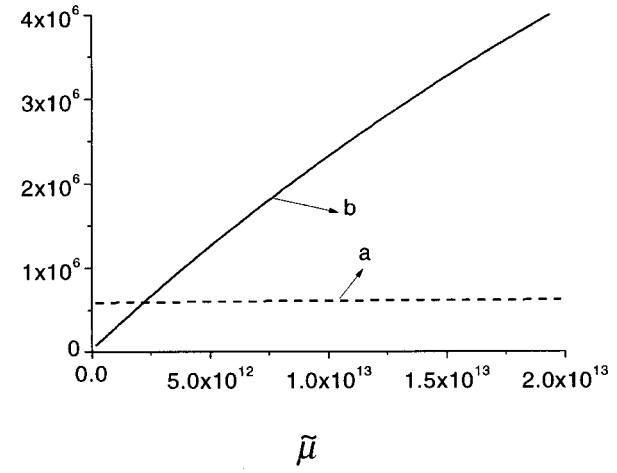

Fig. 7. a, Frequency ω_r of the oscillations and b, damping rate γ_r versus $\tilde{\mu}$.

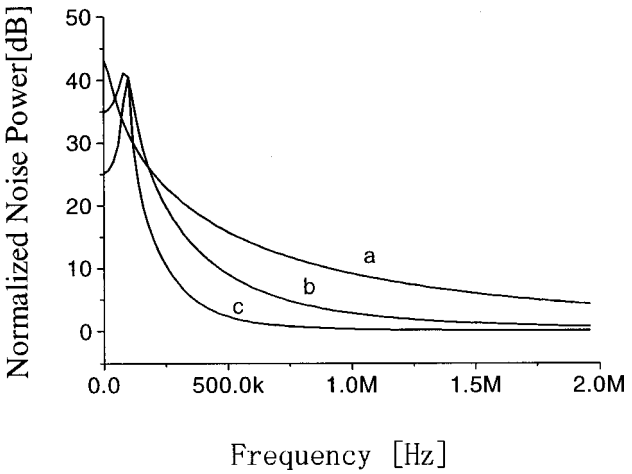

Fig. 8. Harmonic spectra for three values of $\tilde{\mu}$ with $V_{\text{pump}} = 50$ dB: a, $\tilde{\mu} = 10^{13}$; b, $\tilde{\mu} = 10^{12}$; c, $\tilde{\mu} = 10^{11}$.

is commonly dominated by the RRO because $\omega_r' > \gamma_l'$. The frequency of the RRO ω_r and damping rate γ_l of the single-frequency-doubling laser include nonlinear conversion $\tilde{\mu}a_0^2$, so the doubling process will influence the RRO significantly.

The Nd:YVO_4 ring-doubling laser runs in this regime, where $\gamma_s \gg \gamma_t, \Gamma, Ga_0^2$. The parameters of the Nd:YVO_4 ring-doubling laser are listed in Table 1. These parameters were determined in the same way as in the research reported in Ref. 10. The frequency dependence of the second-harmonic output intensity noise is illustrated in Fig. 4, where the second-harmonic intensity noise relative to the QNL is plotted on a log–log scale [$10\log_{10}(V_{\text{out}})$ versus $\log_{10}(\omega/2\pi)$; hence 0 dB indicates that the noise level is equal to the QNL ($V_{\text{out}} = 1$)]. In this figure the intensity-noise level of the second-harmonic output is shown with respect to a QNL pump source ($V_p = 1$). We show the full intensity noise spectrum (curves a) as well as the contributions of the different noise sources to the spectrum (curves b–f). It is clear from Fig. 4 that the intensity-noise spectrum of the harmonic output at the frequency far above ω_r asymptotes to the QNL because of the presence of vacuum fluctuations. The other four noises are small and have no influence at these frequencies. At frequencies near ω_r, chiefly dipole noise and intracavity losses contribute to the spectrum. The noise spectrum can be changed by the intensity-noise level of the pump source shown in Fig. 5. Figure 5 illustrates the main effect of pump noise at a frequency that is obviously below ω_r.

We can alter nonlinear coupling strength $\tilde{\mu}$ by changing the temperature or the matched angle of the optical nonlinear crystal. Figure 6 shows the intracavity photon number of fundamental wave a_0^2 per atom versus $\tilde{\mu}$, according to Eqs. (23)–(26). Frequency ω_r of the oscillations (curve a) and the damping rate γ_L (curve b) are shown in Fig. 7 versus $\tilde{\mu}$. The relative values between ω_r and γ_L are changed relative to $\tilde{\mu}$. So the resonance in the spectrum at frequency ω_r can be changed from the overdamped- to the underdamped driven second-order oscillator according to $\tilde{\mu}$ as shown in Fig. 8. The resonance presents the overdamp at large $\tilde{\mu}$ and the underdamp at small $\tilde{\mu}$. We see that the doubling process can significantly damp the relaxation oscillation.

4. COMPARISON OF THEORETICAL CALCULATION AND EXPERIMENTAL RESULT WITH A Nd:YVO_4 + KTP SINGLE-FREQUENCY-DOUBLING LASER

The experimental setup is shown in Fig. 9. The ring Nd:YVO_4 laser is pumped by a laser diode through an optical coupling system. A transmission cross-coefficient crystal and a half-wave plate are placed in the cavity as an optic diode. A type II critically phase-matched KTP crystal is used to generate the second-harmonic field at 532 nm. The maximum output power obtained is 40 mW, with an optical conversion efficiency of 6%.

The optical signals were detected with a single FND-100 silicon photodiode from EG&G and then amplified by OEI AH0013 and Miteq AU1310 integrated amplifiers. This detector has a large dynamic range and a bandwidth from 10 kHz to 50 MHz. The power spectrum of the signal was recorded with a Hewlett-Packard HP-8590L spectrum analyzer. The saturation characteristics of the photodiodes were checked with as much as 40 mW of optical power incident upon one photodiode. Neither saturation of the dc part nor saturation of the ac noise of the photocurrent at frequencies up to 50 MHz was detected. We calibrated the QNL by detecting the noise spectrum of white-light illumination under the same power level.

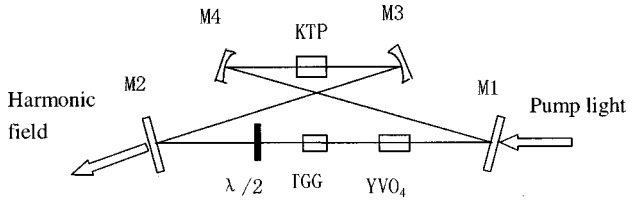

Fig. 9. Experimental setup of a Nd:YVO_4 ring laser for intracavity frequency doubling. M1–M4, mirrors; TGG; terbium gallium garnet crystal.

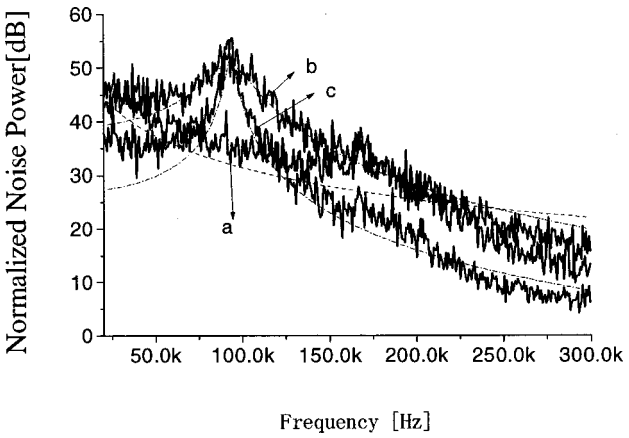

Fig. 10. Harmonic noise spectra with various nonlinear Coupling strengths: a, Intensity noise spectrum of theory and experiment for the 8-mW harmonic output, with the parameter $\tilde{\mu}$ set to $2 \times 10^{13}\,s^{-1}$; b, for the 0.85-mW harmonic output; parameter $\tilde{\mu}$ is set to $1 \times 10^{12}\,s^{-1}$; c, for the 70-μW harmonic output; parameter $\tilde{\mu}$ set to $2 \times 10^{11}\,s^{-1}$.

When the KTP crystal axes are adjusted to a 45° angle with respect to the polarization of the fundamental field, there is a maximum nonlinear conversion efficiency. We can change nonlinear coupling strength $\tilde{\mu}$ by rotating the KTP crystal axes. Figure 10 shows the intensity noise spectra of the harmonic field measured experimentally and the calculation result that w presented in Section 3. Trace a in Fig. 10 is the calculated and measured intensity noise spectrum for the 8-mW harmonic output with a pump power of 0.85 W and its fundamental field linearly polarized at a 45° angle with respect to the KTP crystal axes, trace b is the intensity-noise spectrum for the 0.85-mW harmonic output with same pumped power but with KTP rotated a small angle from 45°, and trace c is the intensity-noise spectrum for the 70-μW harmonic output with same pump power as a result of a larger-angle rotation of KTP. Γ, which corresponds to this pump power, is $6\,s^{-1}$/atom. We found that we obtained the best fit between theory and experiment by setting $V_{\text{pump}} = 500{,}000$, i.e., 57 dB above the QNL. When we measured the intensity-noise level of the laser diode we used a neutral-density filter to reduce the power of the pump field to the level required for the detector. We ensured that all the spatial modes of the laser diode were recorded by focusing the laser radiation onto the photodetectors as tightly as possible. The value of pump noise V_{pump} was obtained from the measured data after optical attenuation was taken into account. We found that the resonance in the spectrum presents an overdamp at large $\tilde{\mu}$ and an underdamp at small $\tilde{\mu}$, which agrees with the theoretical results from the quantum model.

5. CONCLUSION

We have presented an analytical expression for the quantum-noise spectra of a singly resonant active frequency-doubling laser with single-frequency operation obtained by means of the linearized input–output method. This method leads straightforwardly to an analytical expression for the full noise spectra of the output harmonic field. The expression with clearly separated noise terms that stand for the various noise contributions permits greater physical insight into the noise processes, and the result includes the full spectral properties of the pump field and any other input fields, although a maximum of 50% squeezing of the amplitude of the second-harmonic wave is theoretically predicted when there is a high pump rate at zero frequency. Unfortunately, in practical lasers there are large amounts of both pump noise and thermal noise at approximately zero frequency, and the required pump power for squeezing is too great; therefore we know of no experiment with which to demonstrate this type of squeezing. Our calculations showed the influences of various noise sources on the noise spectrum of output field. Reducing the pump noise and increasing pump rate are keys to reaching squeezing. With a practical solid-state laser, the good agreement of experimental and calculated results of the change of resonance in the spectrum from an overdamped- (at higher μ) to an underdamped- (at smaller μ) driven second-order oscillator versus the nonlinear coupling coefficient μ ensures the reliability of our conclusion. The calculated expression can provide useful references for the investigating noise of an active frequency-doubling laser.

ACKNOWLEDGMENTS

This research is supported by the National Natural Science Foundation of China (approvals 69837010 and 19674034), the Excellent Young Teacher Foundation of the Education Department of China and the Shanxi Province Science Foundation.

J. Zhang's e-mail address is jzhang 74@yahoo.com.

REFERENCES

1. K. I. Martin, W. A. Clarkson, and D. C. Hanna, "3 W of single-frequency output at 532 nm by intracavity frequency doubling of a diode-bar-pumped Nd:YAG ring laser," Opt. Lett. **21**, 875–877 (1996).
2. P. J. Hardman, W. A. Clarkson, and D. C. Hanna, "High-power diode-bar-pumped intracavity-frequency-doubling Nd:YLF ring laser," Opt. Commun. **156**, 49–52 (1998).
3. R. Paschotta, M. Collett, P. Kurz, K. Fiedler, H. A. Bachor, and J. Mlynek, "Bright squeezed light from a singly resonant frequency doubler," Phys. Rev. Lett. **72**, 3807–3810 (1994).
4. M. J. Collett and R. B. Leven, "Two-photon-loss model of intracavity second-harmonic generation," Phys. Rev. A **43**, 5068–5072 (1990).
5. C. W. Gardiner and M. J. Collett, "Input and output in damped quantum sustems: quantum stochastic differential equations and master equation," Phys. Rev. A **31**, 3761–3774 (1985).
6. Y. Yamamoto and N. Imoto, "Internal and external field fluctuations of a laser oscillator. I. Quantum mechanical Langevin treatment," IEEE J. Quantum Electron. **QE-22**, 2032–2042 (1986).
7. A. G. White, T. C. Ralph, and H.-A. Bachor, "Active versus passive squeezing by second-harmonic generation," J. Opt. Soc. Am. B **13**, 1337–1346 (1996).
8. J. Maeda, T. Numata, and S. Kogoshi, "Amplitude squeezing from singly resonant frequency-doubling laser," IEEE J. Quantum Electron. **33**, 1057–1067 (1997).

9. Y. Yamamoto, S. Machida, and O. Nilsson, "High-impedance suppression of pump fluctuation and amplitude squeezing in semiconductor lasers," Phys. Rev. A **35**, 5114–5151 (1987).
10. T. C. Ralph, C. C. Harb, and H.-A. Bachor, "Intensity noise of injection locked lasers: quantum theory using a linearised input–output method," Phys. Rev. A **54**, 4359–4369 (1996).
11. C. C. Harb, T. C. Ralph, E. H. Huntington, I. Freitag, D. E. McClelland, and H.-A. Bachor, "Intensity-noise properties of injection-locked lasers," Phys. Rev. A **54**, 4370–4381 (1996).